

Non-Enzymatic Glucose Sensors for Sensitive Amperometric Detection Based on Simple Method of Nickel Nanoparticles Decorated on Magnetite Carbon Nanotubes Modified Glassy Carbon Electrode

Nongyao Nontawong, Maliwan Amatatongchai^{*}, Purim Jarujamrus, Suparb Tamuang and Sanoee Chairam

Department of Chemistry and Center of Excellence for Innovation in Chemistry,
Faculty of Science, Ubon Ratchathani University, Ubon Ratchathani, 34190, Thailand.

*E-mail: maliwan.a@ubu.ac.th, amaliwan@gmail.com

Received: 29 November 2016 / Accepted: 19 December 2016 / Published: 30 December 2016

A sensitive and selective non-enzymatic glucose sensor was developed based on magnetite (Fe_3O_4) and nickel nanoparticles decorated carbon nanotubes (Fe_3O_4 -CNTs-NiNPs). Fe_3O_4 nanoparticles were in situ loaded on the surface of carboxylated multi-walled carbon nanotubes (CNTs-COOH) by a chemical co-precipitation procedure. Nickel nanoparticles (NiNPs) were prepared through reducing nickel chloride by hydrazine hydrate and then decorated on Fe_3O_4 -CNTs using ultra-sonication. The as-prepared Fe_3O_4 -CNTs-NiNPs was characterized using transmission electron microscopy (TEM) and X-Ray Diffraction (XRD). Glucose sensor was fabricated using glassy carbon (GC) coated with Fe_3O_4 -CNTs-NiNPs composites film. Electrochemical investigations indicate that the Fe_3O_4 -CNTs-NiNPs/GC electrode possesses excellent performance in the electrochemical oxidation of glucose at an applied potential of +0.55 V (vs. Ag/AgCl) in 0.1 M NaOH solution. The linear dynamic range for glucose amperometric detection ($E_{\text{app}} = +0.55$ V) was observed from 10 μM to 1.8 mM ($r^2 = 0.998$) with the sensitivity of 335.25 $\mu\text{A mM}^{-1}$; and a low detection limit of 6.7 μM ($S/N = 3$). In addition, the fabricated sensor was successfully applied to determine glucose in honey and energy drinks with good results.

Keywords: Amperometric sensor; carbon nanotubes; magnetite, nickel nanoparticles; glucose

1. INTRODUCTION

Recently, methods for monitoring glucose levels in body fluids for clinical applications, pharmaceutical products and beverages for industrial quality control have received considerable attention. In the previous reports, efforts to develop selective and sensitive methods for the analysis of

glucose include colorimetric [1-5], chemiluminescent [6, 7], and electrochemical approaches [8-15]. These approaches all rely on glucose oxidation reaction catalyzed by enzyme glucose oxidase (GOx). Among these methods, electrochemical detection by a biosensor [8-15] is one of the most commonly used because of inherent high sensitivity and simplicity of instrumentation. Most of the electrochemical glucose biosensors are based on GOx immobilized on a material to prepare glucose sensor. Typically, GOx catalyzes the oxidation of glucose into gluconolactone in the presence of dissolved O_2 with O_2 being reduced to H_2O_2 . Therefore, electrochemical detection of glucose is accomplished by monitoring either O_2 consumption or H_2O_2 production. Another approach has been developed based on direct electrochemistry of GOx using nanomaterials [10, 14, 16]. Although GOx is relatively more stable than other enzymes, use of the biosensor is limited by relatively high cost, inherent stability, complicated immobilization procedures, and certain critical operational and storage conditions e.g. temperature, pH and ionic strength [8, 10, 11, 15].

In contrast, non-enzyme glucose sensors are based on nanostructured metal (Ni) [17, 18], metal alloy (Pt-Pb, Pt-Au) [19, 20] or metal oxides (NiO, MnO_2) [21, 22] as inorganic electrocatalysts using carbon materials such as carbon nanotubes (CNTs) [21, 22] and graphene as scaffolds [18]. This enzyme-free based sensor is an attractive alternative technique to solve the disadvantages of enzymatic biosensors. Quantification of glucose is achieved via directly electrochemical oxidation of glucose at the surface of developed sensors. However, the direct oxidation of glucose based on the mentioned electrodes has a key problem, which is the low sensitivity due to the sluggish kinetics of glucose electro-oxidation [19, 20]. Higher performance for glucose detection has been obtained by using several kind of electrodes contained Ni, NiO or $Ni(OH)_2$ nanocomposites [22-26] compared to the other electrodes. For examples, Lu et al. [23] synthesized Ni nanowire arrays using template-directed electropolymerization strategy with nanopore polycarbonate membrane as a template. $Ni(OH)_2$ nanoflowers for non-enzymatic glucose sensor were synthesized under harsh conditions and high temperature [24]. Sun et al. [25] combined Ni with CNTs to fabricate nanohybrid films on glassy carbon electrode using electrodeposition of $NiCl_2$ and CNTs in ionic liquids. Recently, Choi et al. reported strategy to fabricate CNTs-Ni nanocomposites through atomic layer deposition of Ni followed by chemical vapor deposition of functionalized CNTs [27]. These electrodes showed highly sensitive, selective and satisfactorily stable response towards glucose at low over potential under alkaline condition. However, the methods for synthesized Ni nanostructured or Ni-hybrid materials are somehow relatively complicated. In practice, the high cost of the electrode due to the sophisticated method and expensive instruments may limit their real applications.

This paper describes a simple and effective method for constructing a glucose non-enzymatic sensor using hybrid materials of magnetite (Fe_3O_4) and nickel nanoparticles decorated carbon nanotubes (Fe_3O_4 -CNTs-NiNPs). The combination of CNTs with magnetite and nickel nanoparticles is expected to be an effective electrocatalyst to make glucose sensor. It is well known that CNTs are very hydrophobic and cannot be wetted by liquids possessing a surface tension greater than approximately 100 or 200 mN m^{-1} [28, 29]. Thus, most metals nanoparticles or metal oxide nanoparticles, including Fe_3O_4 and NiNPs, are unable to adhere to the CNTs surface. Our simple and effective strategy to solve this problem is loading Fe_3O_4 nanoparticles in situ on the surface of carboxylated multi-walled carbon nanotubes (CNTs-COOH) via a chemical co-precipitation procedure. After that, NiNPs were decorated

on Fe₃O₄-CNTs using ultra-sonication. Our simple and effective method enables the uniformly deposition of Fe₃O₄ and NiNPs onto the surface of CNTs. We constructed a glucose sensor using the Fe₃O₄-CNTs-NiNPs nanocomposites coated on the surface of glassy carbon electrode. The Fe₃O₄-CNTs-NiNPs/GC electrode shows an excellent activity for the electrocatalysis of glucose oxidation. The fabricated electrode was applied for amperometric detection of glucose in honey and energy drinks with good sensitivity and acceptable selectivity. The developed electrode is found to be a promising enzyme-free glucose sensor.

2. EXPERIMENTAL

2.1 Reagent and Chemical

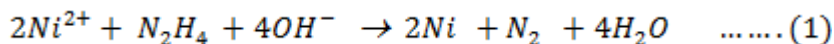
Carboxylated functionalized multiwall carbon nanotubes (CNTs-COOH), diameter: 15 ± 5 nm, with purity of 95%, were purchased from Nanolab Inc (MA, USA). Iron (II) chloride tetrahydrate (FeCl₂·4H₂O), iron (III) chloride hexahydrate (FeCl₃·6H₂O), uric acid (UA), D (+) glucose, ascorbic acid (AA) and dopamine (DA) were purchased from Sigma-Aldrich (St. Louis, USA). Sodium hydroxide (NaOH) and hydrazine hydrate (N₂H₂·N₂H₂·H₂O, 98%) were purchased from Carlo Erba (Val-de-Reuil, France). Ethylene glycol (99.8%, anhydrous) was purchased from Acros organic (Geel, Belgium). All chemicals were of analytical reagent grade and were used without further purification. All solutions were prepared in deionized-distilled water (Water Pro PS, USA).

2.2 Apparatus

Cyclic voltammetric measurements were carried out using an eDAQ potentiostat (model EA 161, Australia) equipped with an e-corder 210 and e-chem v 2.0.13 software. The active surface area of glassy carbon electrode, (diameter 3 mm, CH Instrument, USA) was approximately 0.07 cm². An in house three-electrode cell, comprising a working electrode (Fe₃O₄-CNTs-NiNPs/GC electrode), a reference electrode (Ag/AgCl) and a counter electrode (stainless steel) was employed. Measurements were performed using 0.1 M sodium hydroxide (pH 13.0) as supporting-electrolyte solution and all electrochemical measurements were performed at room temperature. The morphology of nanoparticles and nanocomposites were observed by JEM-1230 transmission electron microscope (TEM; JEOL, Japan). X-ray Diffraction (XRD) analysis of the samples was carried out using a Siemens D5000 diffractometer with Cu K_α monochromatized radiation source, operated at 40 kV and 100 mA.

2.3 Preparation of NiNPs

A method for synthesis of nickel nanoparticles (NiNPs) through reducing nickel chloride by hydrazine hydrate as described by Wu's method [30, 31] was adopted. The reaction mechanism can be described by the following reaction equation,



In brief, 0.952 g of nickel chloride and 5.0 g of hydrazine hydrate were dissolved in 395.0 mL ethylene glycol. Then, 4.0 mL of 1.0 M sodium hydroxide solution was added to the solution. The solution was further stirred in a capped flask for 1 h at 60°C. The obtained black Ni nanoparticles (NiNPS) was washed thoroughly with ethanol and dried at 60°C for 24 h. NiNPs were obtained as a black powder.

2.3 Preparation of Fe₃O₄-CNTs nanocomposites

Fe₃O₄-CNTs nanocomposite was prepared according to a method described previously by Teymourian *et al.* [32] with a slight modification. The nanocomposite was synthesized under N₂ atmosphere. Briefly, 20 mg of carboxylated carbon nanotubes (CNTs-COOH) were dispersed in 20 mL of distilled water in an ultrasonic bath for 20 min. Then 30 mg of FeCl₃·6H₂O was added under vigorous stirring. After the mixture was stirred for 30 min, 40 mg of FeCl₂·4H₂O was added and continued stirring for 30 min. 2 mL of concentrated NH₃ diluted with 10 mL of deionized water was slowly added into the mixture. The solution was then heated at 60°C for another 2 h. Fe₃O₄-CNTs nanoparticles were separated using an external magnetic field, then washed with ethanol and deionized water. After drying in a desiccator, Fe₃O₄-CNTs nanoparticles were obtained as a powder.

2.4 Preparation of the Fe₃O₄-CNTs-NiNPs

Simple method for preparation of Fe₃O₄-CNTs-NiNPs dispersion was firstly proposed in this work. The dispersion was prepared by only dispersing 2 mg of Fe₃O₄-CNTs into 1.0 mL of aqueous solution containing 1% DMF and ultrasonicated for 30 min. After that, 2 mg NiNPs was added into the resulting dispersion and ultrasonicated for 30 min. Finally, homogeneous Fe₃O₄-CNTs-NiNPs dispersion was obtained and the resulting solution was sonicated for 5 min before use.

2.5 Preparation of the Fe₃O₄-CNTs-NiNPs modified GC electrode

Prior to the electrochemical experiments, glassy carbon (GC) electrode was polished using 1.0 and 0.03 μm alumina slurry, successively. The electrode was rinsed with distilled water and sonicated in deionized water of 5 min to remove residual abrasive particles. Fe₃O₄-CNTs-NiNPs/GC electrode was prepared by casting 40 μL of the Fe₃O₄-CNTs-NiNPs dispersion (2 mg mL⁻¹), mentioned above, on the surface of the polished glassy carbon (GC) electrode, and then left to dry at room temperature.

3. RESULTS AND DISCUSSION

3.1 Characterization of the nanomaterials

The morphology and structure of the different composites were studied by TEM and XRD. The TEM samples were prepared by dispersing the nanocomposites in de-ionized water with ultrasonicator and then drying a drop of the suspension on a copper grid. Fig. 1 (A-C) shows TEM

images of (A) the fine nanotubular morphology of CNTs-COOH, (B) a homogenous dispersion of NiNPs and (C) synthesized Fe₃O₄-CNTs-NiNPs. In our work, NiNPs were prepared by reduction of Ni²⁺ by hydrazine in the presence of ethylene glycol, as a stabilizing agent [29]. The average diameter of synthesized NiNPs was 21.6 ± 3.2 nm (count = 50). The TEM image of Fe₃O₄-CNTs-NiNPs (Fig. 1C) shows a typical deposition of Fe₃O₄ and NiNPs on the surface of CNTs' nanotubular structure. The average diameter of the nanoparticles synthesized on CNTs surface was estimated to be 20.3 ± 1.6 nm (count = 50), and the nanoparticles tends to homogeneously dispersed all over the CNTs tubes. Fig. 1D shows the X-ray diffraction patterns of NiNPs, Fe₃O₄-CNTs and Fe₃O₄-CNTs-NiNPs obtained under our synthesis conditions.

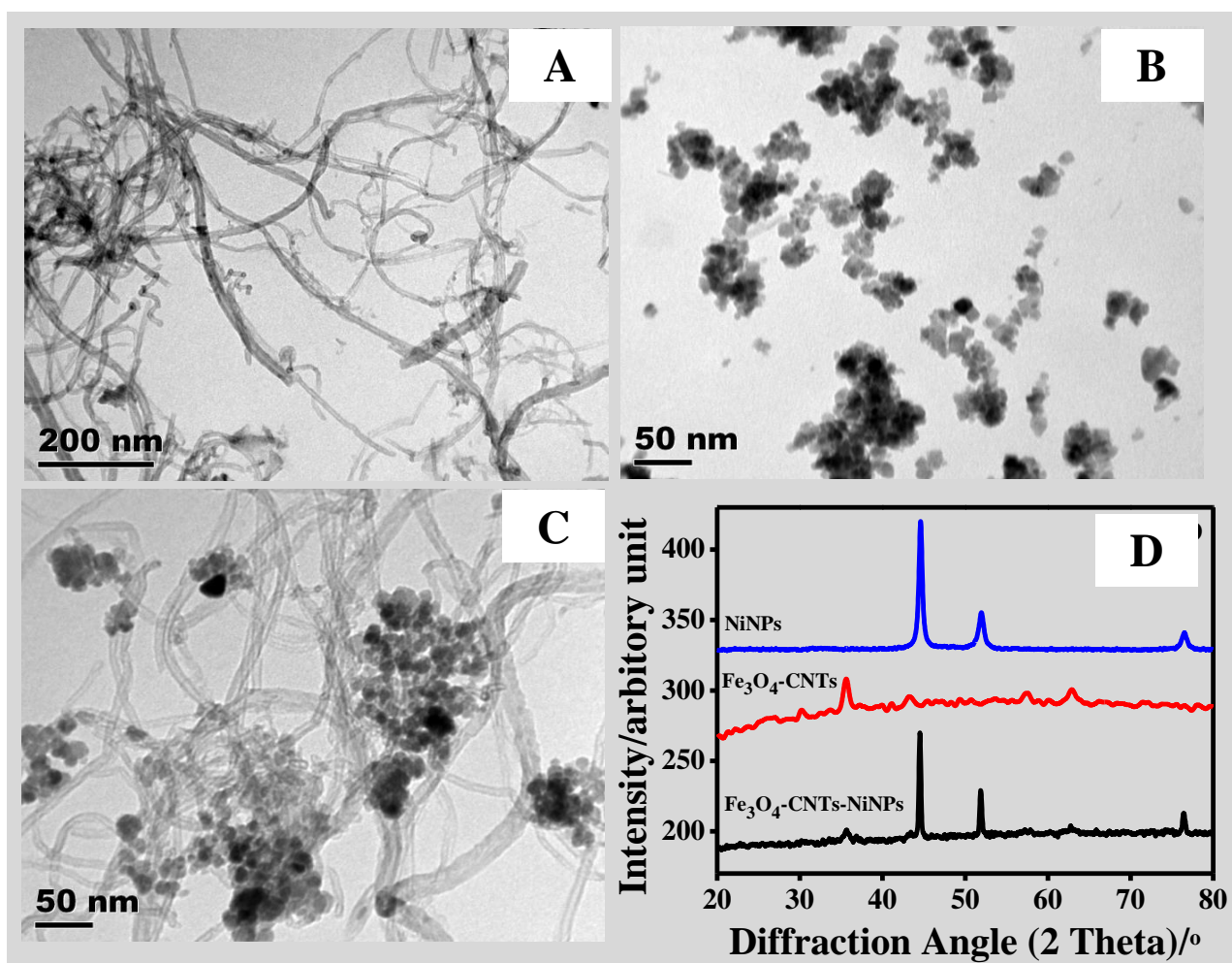


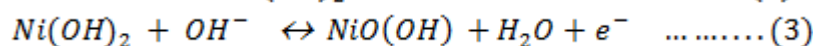
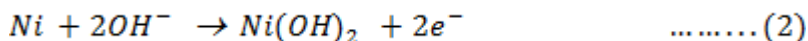
Figure 1. TEM images of (A) CNTs, (B) NiNPs, (C) Fe₃O₄-CNTs-NiNPs and (D) XRD patterns of NiNPs, Fe₃O₄-CNTs and Fe₃O₄-CNTs-NiNPs nanocomposites.

The three well-resolved peaks at 2θ of approximately 44.7° , 52.1° and 76.6° can be assigned to the (111), (200) and (220) planes of pure fcc nickel, which accorded to previous report [30, 31]. This suggests that the as-prepared nanoparticles are nickel nanoparticles. XRD patterns for the Fe₃O₄-CNTs show the peaks at 2θ of approximately 30.4° , 35.7° , 43.6° , 57.8° and 63.4° which were marked by their indices (220), (311), (400), (511) and (440), correspond to the spinel structure of magnetite phase [5,

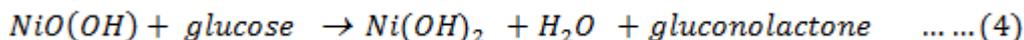
33, 34], (JCPDS No. 82-15330). The XRD pattern of Fe₃O₄-CNTs-NiNPs displays indices corresponding peaks for both NiNPs and Fe₃O₄ which is indicated the formation of Fe₃O₄ and NiNPs decorated on the CNTs.

3.2. Electrochemical behavior of Fe₃O₄-CNTs-NiNPs/GC electrode

Cyclic voltammetry was used to compare and investigate the catalytic activity of the Fe₃O₄-CNTs/GC, NiNPs-CNTs/GC and Fe₃O₄-CNTs-NiNPs/GC electrodes. Fig. 2 shows the cyclic voltammograms (CVs) for different electrodes in 0.1 M NaOH (dash line) with containing 1 mM glucose (solid line). As shown in Fig. 2, no peak was observed on the Fe₃O₄-CNTs/GC while NiNPs-CNTs/GC and Fe₃O₄-CNTs-NiNPs/GC displayed a pair of well-defined redox peak in the potential range of 0-0.8 V, which can be assigned to the electrochemical redox reaction of Ni(II)/Ni(III) couple on the electrode surface in the alkaline medium [27, 35]. However, the electrode modified with only NiNPs produced very small current. The Fe₃O₄-CNTs-NiNPs/GC electrode shows much larger peak currents than that of NiNPs-CNTs/GC electrode. This result reveals that electrochemical performance of the hybrid nanocomposites is greatly enhanced compared to its individual counterparts. Fig. 2C (dotted line), a pair of well-defined redox peaks, an anodic peak at +0.54 V and a cathodic peak at +0.32 V are observed in the absence of glucose. The couple of peaks are corresponding to the Ni(II)/Ni(III), which can be described by the following reactions [27, 35]:



Glucose oxidation is an electrochemically irreversible process. In the presence of glucose, notable enhancement of the oxidation peak current was observed as shown in Fig. 2C (solid line). This enhancement of anodic current is attributed to the electro-oxidation of glucose with the participation of Ni (III), the process mayb be as following:



The electro-catalytic in glucose oxidation by NiNPs in Fe₃O₄-CNTs-NiNPs/GC electrode is accordance to the previous reports of non-enzymatic glucose sensing fabricated from three-dimension porous nickel nanostructure [36], CNTs-nickel nanocomposites [27] and ultrathin Ni(OH)₂ nanoplates [36] synthesized by hydrogen-evolution-assisted electro-deposition [35], atomic layer deposition [27] and pyrolysis melamine foam followed by the microwave process [36].

Herein, we proposed the good electrochemical performance of Fe₃O₄-CNTs-NiNPs nanocomposites, such as large surface area and electrical conductivity, with the electrocatalytic activity of the hybrid nanocomposites towards glucose oxidation. Our method for the preparation of Fe₃O₄-CNTs-NiNPs nanocomposites is very simple using uncomplicated precipitation method and common laboratory equipment. The fabricating process was cost-effective, time-saving and easy to prepare under ultrasonication.

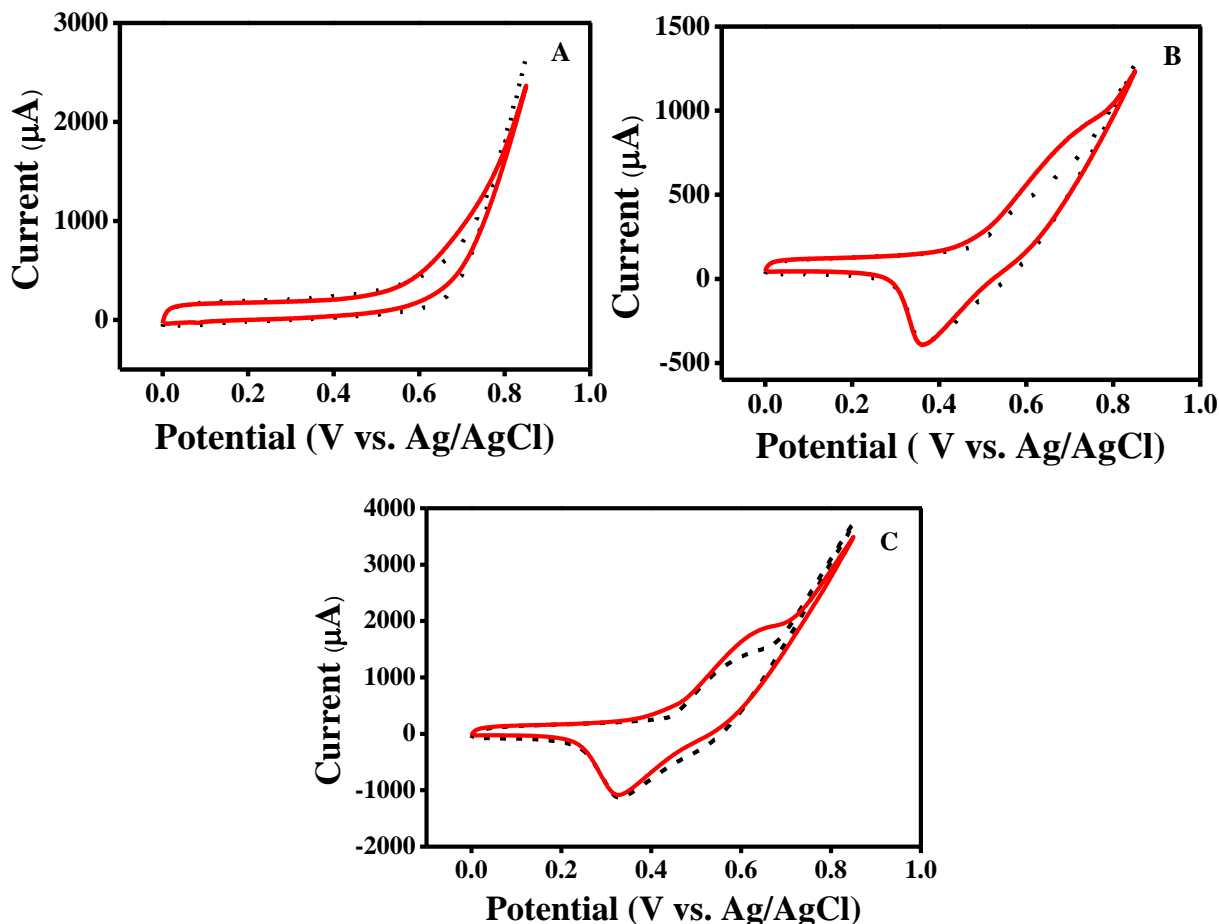


Figure 2. CVs of (A) $\text{Fe}_3\text{O}_4\text{-CNTs/GC}$, (B) NiNPs-CNTs/GC and (C) $\text{Fe}_3\text{O}_4\text{-CNTs-NiNPs/GC}$ electrodes in 0.1 M NaOH, pH 13.0 (dashed line) and in the present of 4 mM glucose (solid line), scan rate 0.05 V s^{-1} .

3.3 Scan rate and concentration dependence study

The influence of scan rate at $\text{Fe}_3\text{O}_4\text{-CNTs-NiNPs/GC}$ electrode was investigated in 0.1 M NaOH solution containing 0.5 mM glucose, the results are displayed in Fig. 3A. As seen in the inset of Fig. 3A, peak currents (μA) for both the oxidation and the reduction were linearly proportional to the square root of scan rate ($\text{V}^{1/2} \text{ s}^{-1/2}$) in the range of $0.03\text{-}0.09 \text{ V s}^{-1}$. The linear regression equations were $I_{p,a} = 2327.55 v^{1/2} + 1.60$ ($r^2 = 0.994$) and $I_{p,c} = -6625.05 v^{1/2} + 487.13$ ($r^2 = 0.993$), respectively. This result indicated a diffusion-controlled process at the $\text{Fe}_3\text{O}_4\text{-CNTs-NiNPs/GC}$ electrode.

Fig. 3B displayed CVs of $\text{Fe}_3\text{O}_4\text{-CNTs-NiNPs/GC}$ electrode with various concentrations of glucose in 0.1 M NaOH solution. It can be observed that by increasing the glucose concentration, the oxidation peak current increased and the potential shifted to a more positive value, demonstrating the good catalytic effect of the Ni(II)/Ni(III) redox couple in glucose oxidation [27, 36]. The relationship between oxidation peak current (μA) and glucose concentration was examined from 1 to 6 mM. Linear calibration ($r^2 = 0.999$) was obtained with the slope of $128.31 \mu\text{A.mM}^{-1}$. These results have demonstrated that the $\text{Fe}_3\text{O}_4\text{-CNTs-NiNPs/GC}$ electrode is appropriate for the quantitation of glucose.

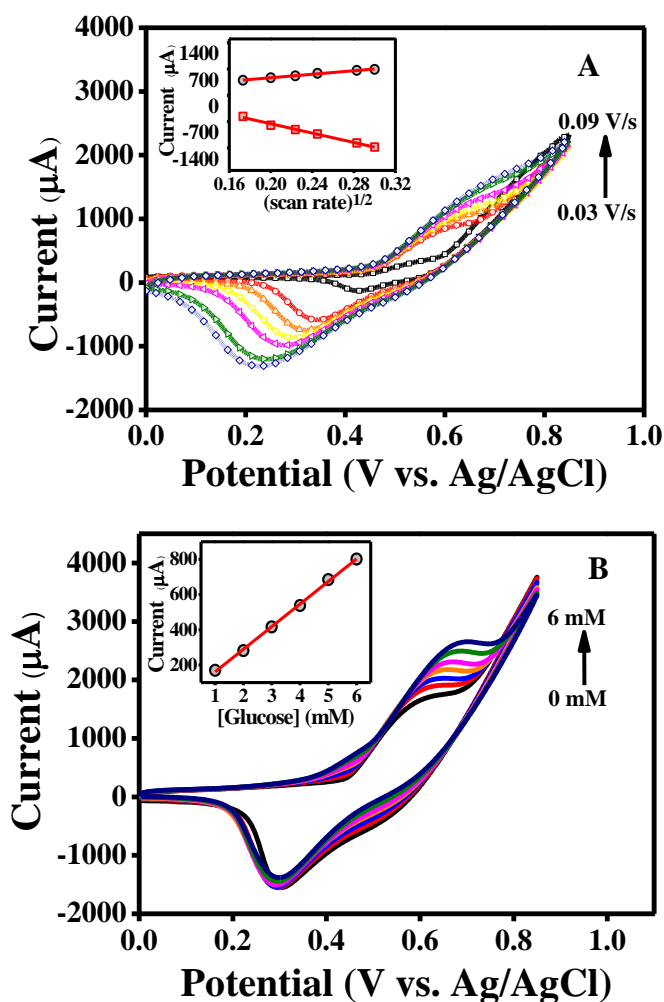


Figure 3. (A) CVs of $\text{Fe}_3\text{O}_4\text{-CNTs-NiNPs/GC}$ electrode for 0.5 mM glucose in 0.1 M NaOH (pH 13) with the variation of scan rate ranging from 0.03 to 0.09 V/s (internal to external). Inset is the plot of the anodic (i_a) and cathodic current (i_c) versus $v^{1/2}$. (B) CVs of glucose in 0.1 M NaOH with the variation of glucose concentration from 0 to 6 mM (internal to external). Inset is the plot of anodic peak currents versus glucose concentration.

3.4 Optimum potential for amperometric detection

The applied potential is an important parameter in amperometry because it strongly affects the size of the current signal from glucose. The proposed amperometric method for detection of glucose was based on the electrochemical monitoring of the oxidation signal from glucose at the $\text{Fe}_3\text{O}_4\text{-CNTs-NiNPs/GC}$ electrode. In this study, we investigated the optimal potential for amperometric detection at the electrode over the potential range from 0.4 to 0.6 V. As shown in Fig. 4, the anodic current response increases rapidly from 0.45 to 0.55 V, and then decreased from 5.5 to 0.7 V. Maximum sensitivity occurred at an operating potential of 0.55 V (versus Ag/AgCl), and thus, we use this optimal voltage for amperometric detection.

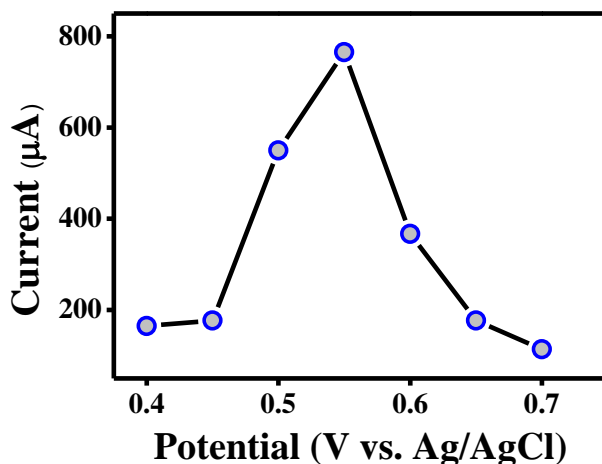


Figure 4. Anodic current of Fe₃O₄-CNTs-NiNPs/GC electrode at different potentials from 0.40 V to 0.70 V upon addition of 1 mM glucose to 0.1 M NaOH.

3.5 Amperometric response of the Fe₃O₄-CNTs-NiNPs /GC electrode to glucose

The amperometric response of the Fe₃O₄-CNTs-NiNPs/GC electrode was investigated by successively addition of glucose standard in a continuous stirring 10 mL of 0.1 M NaOH. Figure 5 displays the amperometric signals corresponding to its calibration plot at optimal potential of +0.55 V. As shown in Fig. 5A, the anodic current increases with increasing the concentration of glucose ranging from 10 µA to 3.0 mM. The Fe₃O₄-CNTs-NiNPs/GC electrode shows very fast current response (~5s) indicated that the electrode is very sensitive to glucose. As shown in Fig. 5B, the linear response range of the developed sensor for glucose concentration was from 10 µM to 1.8 mM with a sensitivity of 335.25 µA mM⁻¹ and correlation coefficient (*r*²) of 0.998. The detection limit estimated based on the signal-to-noise ratio (S/N=3) was 6.7 µM.

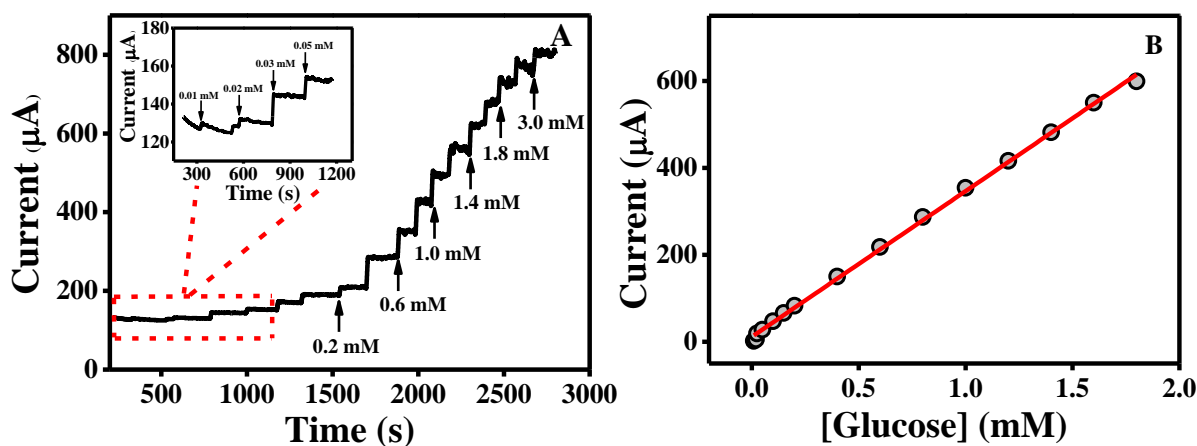


Figure 5. (A) Typical amperometric *i-t* curve of Fe₃O₄-CNTs-NiNPs/GC electrode to successive additions of glucose solution into a stirred system of 0.1 M NaOH (pH 13.0) at +0.55 V. (B) The linear calibration plot of the corresponding current versus glucose concentration.

Table 1. Response characteristics of the Fe₃O₄-CNTs-NiNPs/GC electrode and other non-enzymatic glucose sensors.

Electrode	E _{app} (V)	Sensitivity (μA mM ⁻¹)	Linear range (mM)	Detection limit (μM)	Ref.
MnO ₂ /CNTs ^a	0.30	33.19	0.01-28	-	[22]
RGO-Ni(OH) ₂ ^b	0.54	11.43	0.002-3.1	0.6	[25]
CS-RGO-NiNPs ^c	0.60	318.4	0.2-9	4.1	[18]
Ni/NiO-GP ^c	0.55	1997	0.029-6.4	1.8	[37]
NiO-GP ^b	0.35	7.57	0.02-4.5	5	[38]
Ni(OH) ₂ /TiO ₂ ^d	0.50	192	0.03-14	8	[39]
Ni nanowires ^b	0.55	131.1	0.0005 – 7	0.1	[23]
Ni(OH) ₂ nanoflowers ^b	0.49	265.3	0.1-1.1	0.5	[24]
Cu nanoclusters/CNTs ^b	0.65	17.8	0.0007 – 3.5	0.21	[40]
Ni-CNTs ^b	0.60	67.2	0.003 – 17.5	0.89	[26]
Ni/Cu/CNTs ^b	0.58	186.2	0.00003 – 0.8	0.03	[41]
Fe ₃ O ₄ -CNTs-Ni ^b	0.55	335.3	0.01-1.8	6.7	This work

RGO-Ni(OH)₂ = reduced graphene oxide assembled with Ni(OH)₂ nanoplates, CS = chitosan, RGO = reduced graphene oxide, NiNPs= nickel nanoparticles, GP = Graphene, E_{pp}= applied potential, ^aCarbon nanotubes electrode (CNTsE), ^bGlassy Carbon Electrode (GCE), ^cScreen Printed Electrode (SPE), ^dNiTi alloy sheet

Table 1 provides a comparison of the analytical characteristics of our non-enzymatic glucose sensor with related modified electrodes from the literature. The analytical characteristics of our sensor are comparable to, or better than, those reported for other nanomaterial based-glucose sensor designs. Additionally, the applied potential for our sensor is lower [18, 26, 40], or comparable to, those in previous reports [23, 25, 37, 39, 41]. Moreover, the use of the Fe₃O₄-CNTs-NiNPs/GC electrode offers a higher sensitivity [22-26, 38-41], or comparable [18] to those previously reported values for other modified electrodes. The developed electrode provides a satisfactory wide range of linearity and low detection limit. Our approach to fabricate a sensitive and selective non-enzymatic glucose sensor using glassy carbon (GC) electrode coated with Fe₃O₄-CNTs-NiNPs composites film resulted in high electrocatalytic activity and improved sensor performance toward glucose detection. The synthesis of

Fe_3O_4 -CNTs-NiNPs nanocomposites is very simple by in situ loaded Fe_3O_4 nanoparticles on CNTs via chemical co-precipitation procedure follow by NiNPs decorated on Fe_3O_4 -CNTs-NiNPs via ultrasonication.

3.6 Sensor selectivity reproducibility and stability

Interference studies were conducted to identify specie that may affects the analysis. In this study, we divide samples into two categories of samples containing low matrix such as soft-drinks, honey and syrup and samples containing high matrices e.g. body fluids. To test the possibility of using this method for high matrix samples, we investigated the effects of ascorbic acid (AA), dopamine (DA) and uric acid (UA) that are normally co-existed with glucose in real samples like body fluids. The normal range for blood glucose concentration is about 4.4-6.6 mM, while those of AA, DA and UA are about 0.1 mM [16, 42, 43]. Therefore, the anti-interference performance of the Fe_3O_4 -CNTs-NiNPs/GC electrode against these foreign species was examined. It can be seen that a well-defined glucose response was obtained, while insignificant responses were observed for the interfering species (Fig. 6). Tolerances toward these compounds are satisfied, and negligible interference was observed during testing. We conclude that our proposed electrode provides good selectivity for the amperometric determination of glucose with high potential applicable in clinical diagnostic.

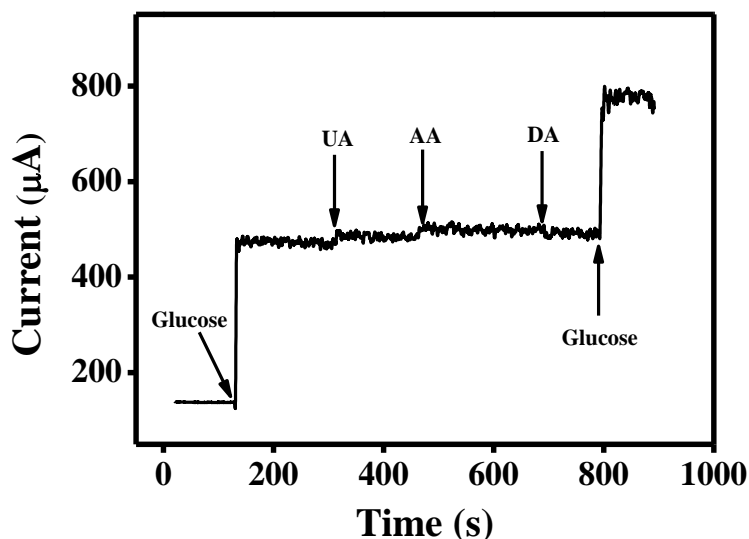


Figure 6. Amperometric response of the Fe_3O_4 /CNTs/NiNPs/GC in 0.1 M NaOH (pH 13) upon the successive addition of 1 mM glucose, 0.5 mM uric acid (UA), 0.1 mM ascorbic acid (AA), 0.01 mM dopamine (DA) and 1 mM glucose, respectively.

To assess the selectivity of the proposed method in sample containing low matrix, we investigated possible interference with glucose detection from competing ions and compounds, such as fructose, maltose, sucrose, carbonic acid, citric acid and sodium chloride, which are always present in energy drinks. We studied the effects of foreign species on the amperometric signals obtained from standard 1 mM glucose. The tolerance limit was taken as the amount of substance needed to cause a

signal alteration of greater than $\pm 5\%$. Tolerance limit for fructose, maltose, sucrose, sodium carbonate, citric acid and sodium chloride was found to be 20, 5, 15, 70, 20 and 100 mM, respectively. Our results demonstrated that different sugars (fructose, maltose and sucrose) and anions (CO_3^{2-} , $\text{C}_6\text{H}_5\text{O}_7^{3-}$ and Cl^-) produce very low interference signals at molar concentration of 5 mM or greater (100 mM) with respect to glucose. However, because samples were diluted between 100 and 1,000 times prior to analysis, the presence of these foreign species is assumed not to be problematic. Thus the selectivity of $\text{Fe}_3\text{O}_4\text{-CNTs-NiNPs/GC}$ electrode for glucose detection was satisfied in the presence of possible interfering reagents and sample ingredients.

Reproducibility and stability experiments were also performed to evaluate the performance of the developed electrode. The electrode-to-electrode reproducibility of $\text{Fe}_3\text{O}_4\text{-CNTs-NiNPs/GC}$ was investigated from the sensitivity or slope of the calibration curve (0.5 to 2.0 mM) of five sensors. As shown in Fig.7, the sensitivity obtained from five electrodes was acquired with a relative standard deviation (RSD) less than 5.0%. The repeatability of the electrode was estimated from six amperometric measurements of 0.5 mM glucose. The sensor shows RSD of 4.13% which indicates that the modified electrode possesses a good stability. This good reproducibility and stability make the developed electrode feasible for practical applications.

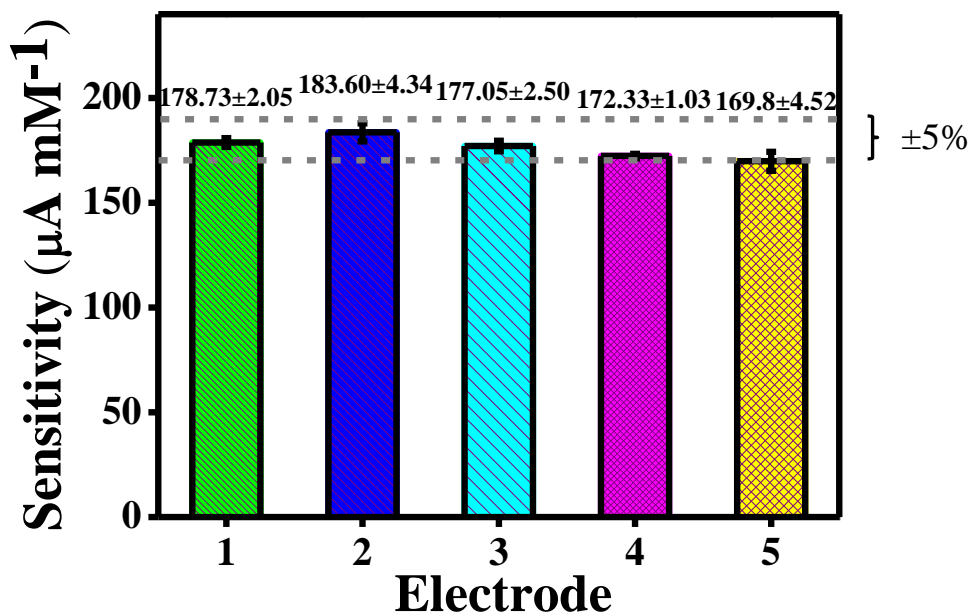


Figure 7 Sensitivity of the calibration curves obtained from five electrodes fabricated independently, concentration of glucose from 0.5 to 2.0 mM.

3.7 Application to energy drinks and honey

In order to test the usefulness of the developed method, $\text{Fe}_3\text{O}_4\text{/CNTs/NiNPs/GC}$ electrode was applied to the determination of glucose in energy drinks and honey. Three different brands of energy drinks (D-1 to D-3) and honey (H-1 to H-3) were analyzed in triplicate by amperometry (Table 2). The samples were diluted appropriately using deionized water prior to the analysis to ensure that the glucose concentrations were within the linear working range and to reduce possible matrix effects.

Glucose content found in D-1 to D-3 by our method is comparable to the label values. Additionally, the results in H-1 to H-3 compare well with measurements obtained from a commercially available glucose meter. The differences between our method and the reference values range from 0.63% to 3.96%, indicating that our test results are in good agreement with those obtained from the drink manufacturers and the glucose meter. These results indicate that our developed method is sufficiently accurate and suitable for the determination of glucose in these samples.

Table 2. Glucose contents found in energy drinks (D-1 to D-3) and honey (H-1 to H-3), which were obtained by the developed method ($\text{Fe}_3\text{O}_4/\text{CNTs}/\text{NiNPs}$ electrode) and comparative values from labeled value and glucose meter. Determination by each method was carried out in triplicate for a sample.

Samples	Glucose content (%w/v)		Developed method (%w/v)	Relative Difference (%)
	Label	Glucose meter		
D-1	8.50		8.63 ± 0.11	+1.53
D-2	8.00		7.91 ± 0.11	-2.38
D-3	4.80		4.83 ± 0.12	+0.63
H-1		20.10	19.27 ± 0.76	+3.96
H-2		15.00	15.46 ± 0.14	+1.95
H-3		8.20	8.35 ± 0.10	+1.83

4. CONCLUSION

A simply new route for the fabrication of sensitive and selective non-enzymatic glucose sensor based on Fe_3O_4 and NiNPs decorated carbon nanotubes ($\text{Fe}_3\text{O}_4\text{-CNTs-NiNPs}$) was proposed. The surface of CNTs-COOH was loaded with Fe_3O_4 nanoparticle via a chemical co-precipitation procedure followed by decorated with NiNPs that prepared through reducing nickel chloride by hydrazine hydrate via ultrasonication. The resulting $\text{Fe}_3\text{O}_4\text{-CNTs-NiNPs}$ nanocomposites were coated on the surface of GC electrode displaying high electrocatalytic activity towards the oxidation of glucose. Thus, the proposed procedure enables simple preparation of non-enzymatic glucose sensor and exhibits high sensitivity, selectivity, stability and reliability using amperometry. Results of glucose measurements in honey and energy drinks using our developed sensor correlated well with those obtained by manufacturer' label and glucose meter.

ACKNOWLEDGEMENTS

The authors gratefully acknowledge financial support received from the National Research Council of Thailand (NRCT, 2560A11702005), the Center of Excellence for Innovation in Chemistry (PERCH-CIC), the Commission on Higher Education, the Ministry of Education, the instrumental facility of the Department of Chemistry, and the Faculty of Science at Ubon Ratchathani University. We also gratefully acknowledge a Scholarship from the Science Achievement Scholarship of Thailand (SAST) that was awarded to N. Nontawong.

References

1. H. Wei and E. Wang, *Anal. Chem.*, 80 (2008) 2250.
2. L. Caseli, D.S. dos Santos Jr, R.F. Aroca and O. N. Oliveira Jr, *Mater. Sci. Eng. C*, 29 (2009) 1687.
3. G. Palazzo, L. Facchini and A. Mallardi, *Sens. Actuators B*, 161 (2012) 366.
4. W. Zhang, D. Ma and J. Du, *Talanta*, 120 (2014) 362.
5. K. Ponlakheth, M. Amatatongchai, W. Sroysee, P. Jarujamrus and S. Chairam, *Anal. Methods*, 8 (2016) 8288.
6. L. Qingwen, L. Guoan, W. Yiming and Z. Xingrong, *Mater. Sci. Eng., C* 11 (2000) 67.
7. C. Wang and H. Huang, *Anal. Chim. Acta*, 498 (2003) 61.
8. J. Wang, S. Li, J.-W. Mo, J. Porter, M. M. Musameh and P. K. Dasgupta, *Biosens Bioelectron.*, 17 (2002) 999.
9. I. Willner and E. Katz, *Angew. Chem. Int. Ed.*, 39 (2000) 1180.
10. V. Mazeiko, A. K. Minkstimiene, A. Ramanaviciene, Z. Belevicius and A. Ramanavicius, *Sens. Actuators, B* 189 (2013) 187.
11. V. Mani, R. Devasenathipathy, S.-M. Chen, B. Subramani and M. Govindasamy, *Int. J. Electrochem. Sci.*, 10 (2015) 691.
12. B. Unnikrishnan, S. Palanisamy and S.-M. Chen, *Biosens Bioelectron.*, 39 (2013) 70.
13. P. Rattanarat, P. Teengam, W. Siangproh, R. Ishimatsu, K. Nakano, O. Chailapakul and T. Imato, *Electroanalysis*, 27 (2015) 703.
14. M. L. Mena, P. Yez-Sedeo and J. M. Pingarrn, *Anal. Biochem.*, 336 (2005) 20.
15. A. Fatoni, A. Numnuam, P. Kanatharana, W. Limbut, C. Thammakhet and P. Thavarungkul, *Sens. Actuators B*, 185 (2013) 725.
16. M. Amatatongchai, W. Sroysee, S. Chairam and D. Nacapricha, *Talanta*, (2016), <http://dx.doi.org/10.1016/j.talanta.2015.11.072>
17. K. E. Toghill, L. Xiao, M. A. Phillips and R. G. Compton, *Sensors. Actuators, B* 147 (2010) 642.
18. J. Yang, J. H. Yu, J. R. Strickler, W. J. Chang and S. Gunasekaran, *Biosens Bioelectron.*, 47 (2013) 530.
19. J. Wang, D. F. Thomas and A. Chen, *Anal. Chem.*, 80 (2008) 997.
20. X. Zhu, C. Li, X. Zhu and M. Xu, *Int. J. Electrochem. Sci.*, 7 (2012) 8522.
21. Y. Mu, D. Jia, Y. He, Y. Miao and H.-L. Wu, *Biosens Bioelectron.*, 26 (2011) 2948.
22. J. Chen, W.-D. Zhang and J.-S. Ye, *Electrochem. Commun.*, 10 (2008) 1268.
23. L. M. Lu, L. Zhang, F. L. Qu, H. X. Lu, X. B. Zhang, Z. S. Wu, S. Y. Huan, Q. A. Wang, G. L. Shen and R. Q. Yu, *Biosens Bioelectron*, 25 (2009) 218.
24. H. Yang, G. Gao, F. Teng, W. Liu, S. Chen and Z. Ge, *J. Electrochem. Soc.*, 161 (2014) B216.
25. Y. Zhang, F. Xu, Y. Sun, Y. Shi, Z. Wen and Z. Li, *J. Mater. Chem.*, 21 (2011) 16949.
26. A. Sun, J. Zheng and Q. Sheng, *Electrochim. Acta*, 65 (2012) 64.
27. T. Choi, S. H. Kim, C. W. Lee, H. Kim, S.-K. Choi, S.-H. Kim, E. Kim, J. Park and H. Kim, *Biosens Bioelectron.*, 63 (2015) 325.
28. S. Hrapovic, Y. Liu, K. B. Male and J. H. T. Luong, *Anal. Chem.*, 76 (2004) 1083.
29. M. Tominaga, T. Shimazoe, M. Nagashima and I. Taniguchi, *Electrochem. Commun.*, 7 (2005) 189.
30. S. H. Wu and D. H. Chen, *J. Colloid Interface Sci.*, 259 (2003) 282.
31. X. Wu, W. Xing, L. Zhang, S. Zhuo, J. Zhou, G. Wang and S. Qiao, *Powder Technol.*, 224 (2012) 162.
32. H. Teymourian, A. Salimi and R. Hallaj, *Biosens Bioelectron.*, 33 (2012) 60.
33. S. Karamipour, M. S. Sadjadi and N. Farhadyar, *Spectrochim. Acta, Part A*, 148 (2015) 146.
34. W. Sroysee, K. Ponlakheth, S. Chairam, P. Jarujamrus and M. Amatatongchai, *Talanta*, 156-157 (2016) 154.
35. X. Niu, M. Lan, H. Zhao and C. Chen, *Anal. Chem.* 85 (2013) 3561.

36. Q. Guo, M. Zhang, S. Liu, G. Zhou, X. Li, H. Hou and L. Wang, *Anal. Methods*, 8 (2016) 8227.
37. X. Zhang, Z. Zhang, Q. Liao, S. Liu, Z. Kanga and Y. Zhang, *Sensors*, 16 (2016) 1791.
38. X. Zhu, Q. Jiao, C. Zhang, X. Zuo, X. Xiao, Y. Liang and J. Nan, *Microchim Acta*, 180 (2013) 477.
39. A. Gao, X. Zhang, X. Peng, H. Wu, L. Bai, W. Jin, G. Wu, R. Hang and P. K. Chu, *Sens. Actuators, B*, 232 (2016) 150.
40. X. Kang, Z. Mai, X. Zou, P. Cai and J. Mo, *Anal. Biochem.*, 363 (2007) 143.
41. K.-C. Lin, Y.-C. Lin and S.-M. Chen, *Electrochim. Acta*, 96 (2013) 164.
42. J. Wang, *Chem. Rev.*, 108 (2008) 814.
43. S. Canivell and R. Gomis, *Autoimmun. Rev.*, 13 (2014) 403.

© 2017 The Authors. Published by ESG (www.electrochemsci.org). This article is an open access article distributed under the terms and conditions of the Creative Commons Attribution license (<http://creativecommons.org/licenses/by/4.0/>).